Vol. 31, No. 9 Journal of Semiconductors September 2010

Analytical charge control model for AlGaN/GaN MIS-HFETs including an undepleted barrier layer

Lu Shenghui(卢盛辉)†, Du Jiangfeng(杜江锋), Luo Qian(罗谦), Yu Qi(于奇), Zhou Wei(周伟),
Xia Jianxin(夏建新), and Yang Mohua(杨谟华)

(State key Laboratory of Electronic Thin Films and Integrated Devices, University of Electronic Science and Technology of China, Chengdu 610054, China)

Abstract: An analytical charge control model considering the insulator/AlGaN interface charge and undepleted AlGaN barrier layer is presented for AlGaN/GaN metal–insulator–semiconductor heterostructure field effect transistors (MIS-HFETs) over the entire operation range of gate voltage. The whole process of charge control is analyzed in detail and partitioned into four regions: I—full depletion, II—partial depletion, III—neutral region and IV—electron accumulation at the insulator/AlGaN interface. The results show that two-dimensional electron gas (2DEG) saturates at the boundary of region II/III and the gate voltage should not exceed the 2DEG saturation voltage in order to keep the channel in control. In addition, the span of region II accounts for about 50% of the range of gate voltage before 2DEG saturates. The good agreement of the calculated transfer characteristic with the measured data confirms the validity of the proposed model.

Key words: AlGaN/GaN; MIS-HFET; 2DEG; analytical charge control model
DOI: 10.1088/1674-4926/31/9/094004 **PACC:** 7280E; 7340L; 7340Q

1. Introduction

AlGaN/GaN metal–insulator–semiconductor heterostructure field effect transistors (MIS-HFETs) have received much attention due to their lower gate leakage current and larger gate voltage swing compared to the conventional Schottky gate HFET (SG-HFET)[1−4]. To evaluate and optimize the performance of AlGaN/GaN MIS-HFETs, a nonlinear charge control model was proposed and used to model the DC and microwave characteristics by Aggarwal *et al.*[5]. On one hand, however, the insulator/AlGaN interface charge which varies for different insulators[4] was not taken into account in this model. On the other hand, the model was derived under the full depletion approximation, thus it is not suitable for the case of undepleted barrier layer which becomes important for large positive gate voltages[6]. Though non-full depletion has been considered in the modeling of AlGaAs/GaAs HFETs[6, 7], the existence of large positive polarization charges at the heterointerface makes the charge control of AlGaN/GaN MIS-HFETs different from that of AlGaAs/GaAs HFETs where the charge control process can be divided into two situations, full depletion and neutral region[6, 7]. In this work, therefore, by comprehensively analyzing the variation of charge distribution in the barrier layer with gate bias, the charge control process over the entire operation voltage range is partitioned into four regions: I—full depletion, II—partial depletion, III—neutral region, IV—electron accumulation at the insulator/AlGaN interface. Then, based on MIS theory and the Poisson equation, the charge control model including the insulator/AlGaN interface charge and undepleted barrier layer is developed. The transfer characteristic based on the present model is in good agreement with the measured data, which means that it is helpful to understand the device physics, optimize the design and evaluate the performance.

2. Analysis of charge control

The schematic of a typical AlGaN/GaN MIS-HFET is shown in Fig. 1. It consists of SiC substrate, an undoped GaN buffer layer, an n-doped AlGaN barrier layer of thickness d and doping concentration N_{D}, and an insulator of thickness t_{Ins} and dielectric permittivity $\varepsilon_{\mathrm{Ins}}$ beneath the metal gate. It is assumed that the positive polarization charge at the heterointerface and the net charge (the sum of negative polarization charge and interface trapped charge) at the insulator/AlGaN interface are σ_{PI} and Q_{Ins}, respectively. The trapped charges in AlGaN, GaN and the insulator are not considered.

The Poisson equation in the AlGaN layer is given by[8, 9]

$$\frac{\mathrm{d}^2 V(x)}{\mathrm{d}x^2} = -\frac{\rho(x)}{\varepsilon} = -\frac{q[N_{\mathrm{D}}^{+}(x) - n(x)]}{\varepsilon}, \tag{1}$$

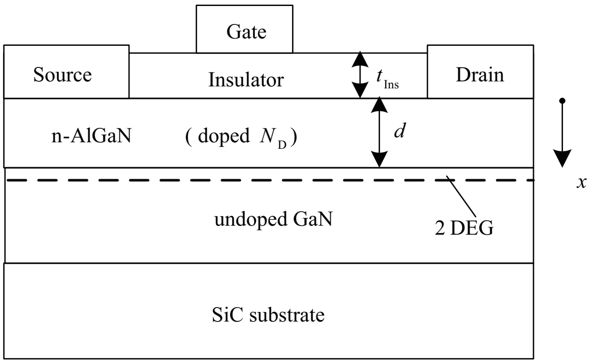

Fig. 1. Schematic of an AlGaN/GaN MIS-HFET.

---

† Corresponding author. Email: lushenghui@sohu.com

Received 9 March 2010, revised manuscript received 7 April 2010

$$N_{\rm D}^{+}(x)=\frac{N_{\rm D}}{1+2\exp[(E_{\rm D}-V(x))/kT]},\tag{2}$$

$$n(x)=\frac{N_{\rm C}}{0.27+\exp[V(x)/kT]},\tag{3}$$

with the boundary conditions:

$$V(x=d)=\Delta E_{\rm C}-E_{\rm F},\tag{4}$$

$$F(x=d^{-})=-(\sigma_{\rm PI}-qn_{\rm s})/\varepsilon,\tag{5}$$

where x is the coordinate in a direction perpendicular to the insulator/AlGaN interface with its origin at the insulator/AlGaN interface, a positive value in the AlGaN layer. $V(x)$ is the conduction band potential, $N_{\rm D}^{+}(x)$ is the ionized donor concentration, $n(x)$ is the free electron concentration, ε is the dielectric constant of AlGaN, $E_{\rm D}$ is the donor energy level below the conduction band, $N_{\rm C}$ is the effective density of states of AlGaN, $\Delta E_{\rm C}$ is the conduction band discontinuity at the heterointerface, F is the electric field, $n_{\rm s}$ is the sheet electron density of two-dimensional electron gas (2DEG), and $E_{\rm F}$ is the Fermi level, which can be approximated as a nonlinear function of $n_{\rm s}$ in the form of a simple polynomial[10]:

$$E_{\rm F}=k_1+k_2n_{\rm s}^{1/2}+k_3n_{\rm s},\tag{6}$$

where k_1 = –0.0984 V, $k_2 = 1.621\times10^{-9}$ V·m, and $k_3 = 1.521\times10^{-18}$ V·m^2 are found afresh for the AlGaN/GaN system using the effective mass of an electron $m^* = 0.22m_0$.

The Poisson equation above can only be solved numerically, so some approximations must be adopted to achieve a simple analytical model according to the charge distribution in the AlGaN barrier layer. The insulator/AlGaN interface charge is not taken into account in this section since it can be ascribed to the flatband voltage of MIS structure in the next section.

2.1. Region I: full depletion

When gate bias is low in an AlGaN/GaN MIS-HFET, the AlGaN layer is fully depleted by the gate, so the electric lines of force starting from ionized donor positive charges point to the gate. In addition, some of the lines of force from positive polarization charges also point to the gate and the others terminate at the channel. Figure 2(a) shows the charge distribution and conduction band diagram. Due to full depletion, we get $N_{\rm D}^{+}(x) = N_{\rm D}$ and $n(x) = 0$ for the entire barrier layer. Hence the Poisson equation (1) can be simplified as

$$\frac{{\rm d}^2V(x)}{{\rm d}x^2}=-\frac{qN_{\rm D}}{\varepsilon}.\tag{7}$$

According to the charge neutrality condition, the gate charge $Q_{\rm G}$ induced by the net charge of the semiconductor side can be expressed as

$$Q_{\rm G}=-[\sigma_{\rm PI}+qN_{\rm D}d-qn_{\rm s}].\tag{8}$$

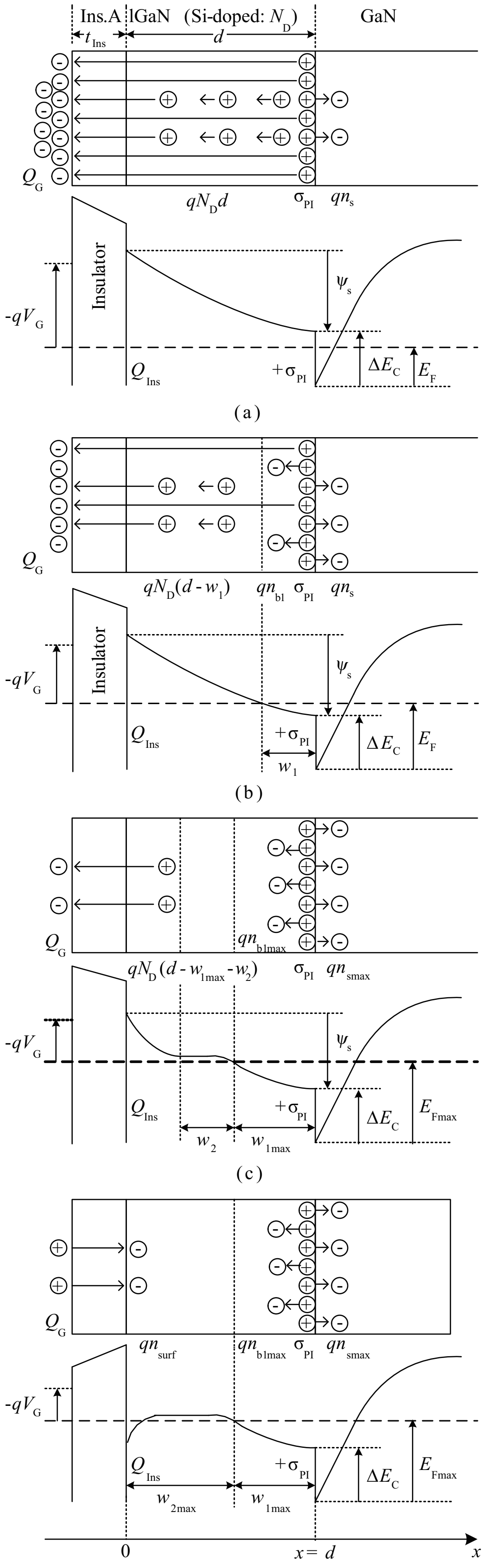

Fig. 2. Charge distribution sketch maps and conduction band diagrams of an AlGaN/GaN MIS-HFET for regions (a) I, (b) II, (c) III and (d) IV.

2.2. Region II: partial depletion

With the increase of gate voltage in region I, some of the electric lines of force starting from positive polarization charges and pointing to the gate change their directions and point to the channel so that n_s increases and E_F rises. Once n_s is bigger than the 2DEG electron density at $E_F = \Delta E_C$, E_F exceeds ΔE_C, the conduction band of part of AlGaN is below E_F when $N_D^+(x)$ and $n(x)$ nearby the AlGaN side of heterojunction become non-negligible. Thus, the full depletion approximation of AlGaN layer is no longer valid. (Here, $E_F = \Delta E_C$ is approximately regarded as the boundary condition between regions I and II.) Since σ_{PI}/q is much larger than n_s at $E_F = \Delta E_C$, some electric lines of force from polarization charges end at the electrons in AlGaN except for the gate and channel when $E_F > \Delta E_C$. (A detailed discussion about ΔE_C and polarization charge can be found in Ref. [11].) A charge distribution sketch map and conduction band diagram of region II are shown in Fig. 2(b).

In Fig. 2(b) the conduction band of AlGaN intersects the Fermi level at $x = d - w_1$. Assuming the region $0 \leqslant x < d - w_1$ is fully depleted and the donors do not ionize for $d - w_1 \leqslant x \leqslant d$, we have:

$$\begin{cases} N_D^+(x) = N_D \text{ and } n(x) = 0, & 0 \leqslant x < d - w_1, \\ N_D^+(x) = 0, & d - w_1 \leqslant x \leqslant d. \end{cases} \tag{9}$$

The electron concentration at the boundaries can be achieved as from Eq. (3).

$$n_1 = n(x = d - w_1) = \frac{N_C}{1.27}, \tag{10}$$

$$n_2 = n(x = d) = \frac{N_C}{0.27 + \exp[(\Delta E_C - E_F)/kT]}. \tag{11}$$

Furthermore, as an approximation of Eq. (3) for $d - w_1 \leqslant x \leqslant d$, the following linear distribution starting from n_1 and ending at n_2 is adopted:

$$n(x) = \frac{n_2 - n_1}{w_1}[x-(d-w_1)]+n_1, \quad d-w_1 \leqslant x \leqslant d. \tag{12}$$

Substituting Eqs. (9) and (12) into Eq. (1) yields:

$$\frac{d^2V(x)}{dx^2} = \begin{cases} -\dfrac{qN_D}{\varepsilon}, & 0 \leqslant x < d - w_1, \\ \dfrac{q(n_2 - n_1)}{w_1}[x - (d - w_1)] + qn_1, & \\ \quad d - w_1 \leqslant x \leqslant d. & \end{cases} \tag{13}$$

Integrating Eq. (12) from $d - w_1$ to d, the sheet electron density in undepleted AlGaN can be achieved as

$$n_{b1} = \int_{d-w_1}^{d} n(x)dx = \frac{(n_2 + n_1)w_1}{2}. \tag{14}$$

According to the charge neutrality condition, the gate charge Q_G induced by the net charge of the semiconductor side in region II can be expressed as

$$Q_G = -[\sigma_{PI} + qN_D(d - w_1) - qn_s - qn_{b1}]. \tag{15}$$

2.3. Region III: neutrality region

With increasing gate bias, the quality of electric lines of force starting from positive polarization charges pointing to the gate decreases continuously, the electrons in the channel and AlGaN increase and E_F rises. When the number of lines pointing to the gate becomes zero, the sum of negative charge in the channel and AlGaN equals the polarization positive charge, that is:

$$\sigma_{PI} = qn_s + \int_0^d \rho(x)dx \,\big|_{\rho(x)<0} = qn_s + qn_{b1}. \tag{16}$$

At this point, n_s, E_F and w_1 reach their maxima n_{smax}, E_{Fmax} and w_{1max}, respectively. After that, a continuous raising gate voltage results that the region $0 \leqslant x < d - w_{1max}$ cannot be fully depleted by the gate and the neutral region occurs. So the boundary condition between regions II and III is n_s reaching its maximum. A charge distribution sketch map and conduction band diagram of region III are shown in Fig. 2(c). Assuming the width of the neutral region is w_2 and the region $0 < x < d - w_{1max} - w_2$ is fully depleted, we have $N_D^+(x) = N_D$ and $n(x) = 0$ for this region. Hence the Poisson equation (1) can be simplified as

$$\frac{d^2V(x)}{dx^2} = -\frac{qN_D}{\varepsilon}, \quad 0 \leqslant x < d - w_{1max} - w_2. \tag{17}$$

The sheet free electron density in the neutral region is:

$$n_{b2} = N_D w_2. \tag{18}$$

According to the charge neutrality condition, the gate charge Q_G induced by the net charge of the semiconductor side in region III can be expressed as

$$Q_G = -qN_D(d - w_{1\max} - w_2). \tag{19}$$

2.4. Region IV: electron accumulation at the insulator/AlGaN interface

After the neutral region extends to the insulator/AlGaN interface, the raising gate voltage results in electrons accumulating at the insulator/AlGaN interface so that the conduction band bends downward as shown in Fig. 2(d). Therefore, the boundary condition between regions III and IV is w_2 reaching its maximum $w_{2max} = d - w_{1max}$. The increment of gate bias drops across the insulator like a common MIS capacitor, so the electron density accumulating at the insulator/AlGaN interface, n_{surf}, can be evaluated as

$$n_{surf} = C_{Ins}\Delta V_G/q, \tag{20}$$

where $C_{Ins} = \varepsilon_{Ins}/t_{Ins}$ is the insulator capacitance, and ΔV_G is the increment of gate voltage.

3. Analytical charge control model

According to MIS theory, the gate voltage V_G, the flatband voltage V_{FB} and the potential dropping across insulator V_{Ins} can be expressed as

$$V_G = V_{FB} + V_{Ins} + \psi_s, \quad (21)$$

$$V_{FB} = \phi_m - \phi_s - \frac{Q_{Ins}}{C_{Ins}}, \quad (22)$$

$$V_{Ins} = \frac{Q_G}{C_{Ins}}, \quad (23)$$

where ψ_s is the semiconductor surface potential, ϕ_m and ϕ_s are the work functions of gate metal and AlGaN respectively, Q_{Ins} is the insulator/AlGaN interface charge, C_{Ins} is the insulator capacitance, and Q_G is the gate charge induced by that of the semiconductor side.

From Figs. 2(a) or 2(b), the work function of AlGaN can be obtained as

$$\phi_s = \chi + \Delta E_C - E_F, \quad (24)$$

where χ is the electron affinity of AlGaN. Combining Eqs. (21) – (24) yields:

$$V_G = \phi_m - \chi - \Delta E_C + E_F - \frac{Q_{Ins}}{C_{Ins}} + \frac{Q_G}{C_{Ins}} + \psi_s. \quad (25)$$

The surface electric field of AlGaN for the MIS-HFET can be written as

$$F(x = 0^+) = \frac{Q_G}{\varepsilon}. \quad (26)$$

3.1. Region I

Solving the Poisson equation (7) with Eq. (26), we can get:

$$\psi_s = \frac{Q_G}{C_b} + \frac{qN_D d^2}{2\varepsilon}, \quad (27)$$

where $C_b = \varepsilon / d$ is the AlGaN layer capacitance. Substituting Eq. (27) into Eq. (25) and rearranging yields:

$$V_G = \phi_m - \chi - \Delta E_C + E_F - \frac{Q_{Ins}}{C_{Ins}} + \frac{Q_G}{C_t} + \frac{qN_D d^2}{2\varepsilon}, \quad (28)$$

where C_t is the total capacitance from gate to channel, and $1/C_t = 1/C_{Ins} + 1/C_b$. Substituting Eq. (8) into Eq. (28) and rearranging, the charge control model for region I can be obtained as

$$qn_s = C_t (V_G - V_{TH} - E_F), \quad (29)$$

$$V_{TH} = \phi_m - \chi - \Delta E_C - \frac{Q_{Ins}}{C_{Ins}} - \frac{\sigma_{PI}}{C_t} - \frac{qN_D d}{C_t} + \frac{qN_D d^2}{2\varepsilon}, \quad (30)$$

where V_{TH} is the threshold voltage.

3.2. Region II

In Fig. 2(b), the surface potential can be expressed as

$$\psi_s = V(0, d - w_1) + V(d - w_1, d), \quad (31)$$

where the potential differences $V(0,\, d - w_1)$ and $V(d - w_1,\, d)$ can be achieved by solving the Poisson equation (13) with Eq.(26) as

$$V(0, d - w_1) = \frac{Q_G}{\varepsilon}(d - w_1) + \frac{qN_D}{2\varepsilon}(d - w_1)^2. \quad (32)$$

$$V(d - w_1, d) = \Delta E_C - E_F = \left[\frac{Q_G}{\varepsilon} + \frac{qN_D(d - w_1)}{\varepsilon}\right] \times w_1 - \frac{q(n_2 + 2n_1)}{6\varepsilon} w_1^2. \quad (33)$$

From Eqs. (25) and (31)–(33), we can get:

$$V_G = \phi_m - \chi - \Delta E_C + E_F - \frac{Q_{Ins}}{C_{Ins}} + \frac{Q_G}{C_t} + \frac{qN_D(d - w_1)}{2\varepsilon} - \frac{q(n_2 + 2n_1)w_1^2}{6\varepsilon}. \quad (34)$$

Combining Eqs. (14), (15) and (34), the charge control model for region II is obtained as

$$qn_s = C_t\left\{V_G - V_{TH} - E_F - \left[\frac{qN_D w_1}{C_t} + \frac{q(n_1 + n_2)w_1}{2C_t} - \frac{qN_D w_1^2}{2\varepsilon} - \frac{q(n_2 + 2n_1)w_1^2}{6\varepsilon}\right]\right\}. \quad (35)$$

It is noted that Eq. (35) becomes Eq. (29) by setting the width of the undepleted region w_1 to zero.

From Eqs. (14), (15) and (33), we can achieve:

$$\frac{q(2n_2 + n_1)}{6\varepsilon} w_1^2 + \frac{qn_s - \sigma_{PI}}{\varepsilon} w_1 + E_F - \Delta E_C = 0. \quad (36)$$

Solving Eq. (36) yields:

$$w_1 = \frac{-B - \sqrt{B^2 - 4AC}}{2A}, \quad (37)$$

where $A = \frac{q(2n_2+n_1)}{6\varepsilon}$, $B = \frac{qn_s-\sigma_{PI}}{\varepsilon}$, $C = E_F - \Delta E_C$. It is obvious that w_1 reaches its maximum w_{1max} when

$$B^2 - 4AC = 0. \quad (38)$$

We can achieve n_{smax} and E_{Fmax} by solving Eqs. (38), (6), (10) and (11) so that w_{1max} can be obtained from Eq. (37).

3.3. Region III

In Fig. 2(c), the surface potential can be approximated as

$$\psi_{\mathrm{s}} \approx V(0, d - w_{1\max} - w_2) + \Delta E_{\mathrm{C}} - E_{\mathrm{F}\max}, \qquad (39)$$

where the potential difference $V(0, d - w_{1\max} - w_2)$ can be obtained by solving the Poisson equation (17) with Eqs. (26) and (19) as

$$V(0, d - w_{1\max} - w_2) = -\frac{qN_{\mathrm{D}}}{2\varepsilon}(d - w_{1\max} - w_2)^2. \qquad (40)$$

From Eqs. (25), (39) and (40), the relation between gate voltage V_{G} and the width of the neutral region w_2 can be achieved as

$$V_{\mathrm{G}} = \phi_{\mathrm{m}} - \chi - \frac{Q_{\mathrm{Ins}}}{C_{\mathrm{Ins}}} - \frac{qN_{\mathrm{D}}(d - w_{1\max} - w_2)}{C_{\mathrm{Ins}}} - \frac{qN_{\mathrm{D}}(d - w_{1\max} - w_2)^2}{2\varepsilon}. \qquad (41)$$

Combining Eqs. (41) and (18), the charge control model for region III can be obtained as

$$n_{\mathrm{b2}} = N_{\mathrm{D}}\left\{d - w_{1\max} - \left[-\frac{\varepsilon}{C_{\mathrm{Ins}}} + \sqrt{\left(\frac{\varepsilon}{C_{\mathrm{Ins}}}\right)^2 - \frac{2\varepsilon}{qN_{\mathrm{D}}}\left(V_{\mathrm{G}} - \phi_{\mathrm{m}} + \chi + \frac{Q_{\mathrm{Ins}}}{C_{\mathrm{Ins}}}\right)}\right]\right\}. \qquad (42)$$

Substituting the maximum of w_2, $w_{2\max} = d - w_{1\max}$, into Eq. (41), the maximal gate bias of region III is determined as

$$V_{\mathrm{G3}\max} = \phi_{\mathrm{m}} - \chi - \frac{Q_{\mathrm{Ins}}}{C_{\mathrm{Ins}}}. \qquad (43)$$

3.4. Region IV

When $V_{\mathrm{G}} > V_{\mathrm{G3max}}$, the charge control model can be achieved by substituting the increment of gate voltage ($\Delta V_{\mathrm{G}} = V_{\mathrm{G}} - V_{\mathrm{G3max}}$) into Eq. (20) as

$$n_{\mathrm{surf}} = C_{\mathrm{Ins}}(V_{\mathrm{G}} - V_{\mathrm{G3}\max})/q. \qquad (44)$$

According to the discussion above, the free electron includes two parts, one in the channel and the other in AlGaN. The sheet electron density in AlGaN consists of n_{b1}, n_{b2} and n_{surf}. So, the total drain saturation current can be simply evaluated as

$$\begin{aligned} I_{\mathrm{DS}} &= I_{\mathrm{2DEG}} + I_{\mathrm{AlGaN}} \\ &= qn_{\mathrm{s}}v_{\mathrm{sat\_GaN}}W_{\mathrm{G}} + (qn_{\mathrm{b1}} + qn_{\mathrm{b2}} + qn_{\mathrm{surf}})v_{\mathrm{sat\_AlGAN}}W_{\mathrm{G}}, \end{aligned} \qquad (45)$$

where I_{2DEG} and I_{AlGaN} are the saturation currents through the channel and AlGaN barrier layer respectively, $v_{\mathrm{sat\_GaN}}$ and $v_{\mathrm{sat\_AlGaN}}$ are the electron saturation velocities in GaN and AlGaN, respectively, and W_{G} is the gate width. The extrinsic gate voltage can be obtained as

$$V_{\mathrm{GB}} = V_{\mathrm{G}} + I_{\mathrm{DS}}R_{\mathrm{S}}, \qquad (46)$$

where R_{S} is the source contact resistance.

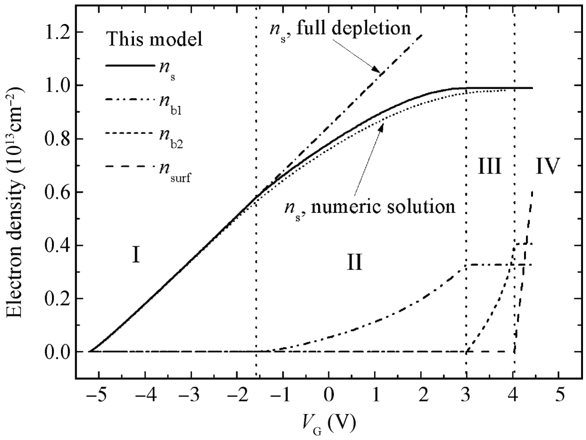

Fig. 3. Variation of n_{s}, n_{b1}, n_{b2}, and n_{surf} with the gate bias.

4. Results and discussion

The AlGaN/GaN MIS-HFET structure fabricated by Yue *et al.*[3] is used to validate the present model. The material and device parameters are listed in Table 1. Wherever possible, actual experimental or theoretical data are adopted except for Q_{Ins} μ_{AlGaN} and $v_{\mathrm{sat\_GaN}}$, which are fitted.

Figure 3 shows the variation of the sheet carrier densities n_{s}, n_{b1}, n_{b2} and n_{surf} with the gate voltage. It can be seen that in region I n_{s} rises fast and there are no free electrons in AlGaN due to full depletion. As the barrier layer is no longer depleted and the electrons begin to accumulate at the AlGaN side of the heterojunction in region II, the increasing speed of n_{s} gradually becomes slow and finally 2DEG saturates. In region III n_{b2} rises in virtue of the extension of the neutral region with gate voltage. In region IV n_{surf} increases rapidly as the increment of gate bias induces the electron accumulation at the insulator/AlGaN interface like a capacitor. After 2DEG saturates, the increasing gate bias can only affect the electrons in AlGaN and the gate loses control of the channel. Therefore, the gate voltage should not exceed the 2DEG saturation voltage in order to keep the channel in control.

It is obvious that the model based on full depletion approximation is not suitable after region I. Compared to the numeric solution, the 2DEG electron density is only slightly overestimated by the present model, which results from the analytical charge distribution in the barrier layer approximating the numeric results as shown in Fig. 4.

In Fig. 3 n_{s} reaches its maximum at V_{G} = 3 V when n_{smax} = 9.89×10^{12} cm^{-2}, w_{1max} = 4.73 nm and n_{b1max} = 3.27×10^{12} cm^{-2}. The sum of n_{smax} and n_{b1max} is 1.316×10^{13} cm^{-2} and it is slightly less than the polarization charge density (σ_{PI}/q = 1.387×10^{13} cm^{-2}), which is attributed to a series of approximations of charge distribution in AlGaN.

Figure 5 shows the variation of n_{smax} and n_{b1max} with Al mole fraction compared to σ_{PI}/q and n_{s} ($E_{\mathrm{F}} = \Delta E_{\mathrm{C}}$). The maximal 2DEG electron densities calculated by our analytical model fit well with the numeric results. The n_{smax} increases rapidly with Al content and it can reach 1.51×10^{13} cm^{-2} for m = 0.4 while the n_{b1max} shows low sensitivity to Al mole fraction. Therefore, in order to achieve the highest value of n_{smax}, the value of m should be as high as possible. However, high Al content may cause the polarization charge to reduce due to the

Table 1. Relevant material and device parameters used in calculation.

Parameter	Symbol	Value	Unit	Ref.
Al content in AlGaN	m	0.3		[3]
AlGaN layer thickness	d	25	nm	[3]
Donor concentration in AlGaN	N_D	2×10^{18}	cm^{-3}	[3]
Gate length	L_G	0.8	μm	[3]
Gate width	W_G	60	μm	[3]
Insulator		Al_2O_3		[3]
Permittivity of insulator	ε_{Ins}	10	ε_0	[3]
Insulator layer thickness	t_{Ins}	3.5	nm	[3]
Electron mobility in GaN	μ_{GaN}	1150	$cm^2/(V \cdot s)$	[3]
Gate metal		Ni/Au		[3]
Work function of Ni & Au	ϕ_m	5.2	eV	[12]
Source contact resistance	R_S	0.8	$\Omega \cdot$mm	[13]
Permittivity of AlGaN	ε	$9.0m + 9.5(1 - m)$	ε_0	[14]
Electron affinity in AlGaN	χ	$1.9m + 3.4(1 - m)$	eV	[15]
Effective density of states of AlGaN	N_C	$4.10 \times 10^{18} m + 2.65 \times 10^{18} (1 - m)$	cm^{-3}	[15]
Electron mobility in AlGaN	μ_{AlGaN}	50	$cm^2/(V \cdot s)$	Fitted
Electron saturation velocity in GaN	v_{sat_GaN}	5.2×10^6	cm/s	Fitted
Charge density at insulator/AlGaN interface	Q_{Ins}	-3.33×10^{13}	qC/cm^2	Fitted
Electron saturation velocity in AlGaN	v_{sat_AlGaN}	$v_{sat\_GaN} / \mu_{GaN} \times \mu_{AlGaN}$	cm/s	

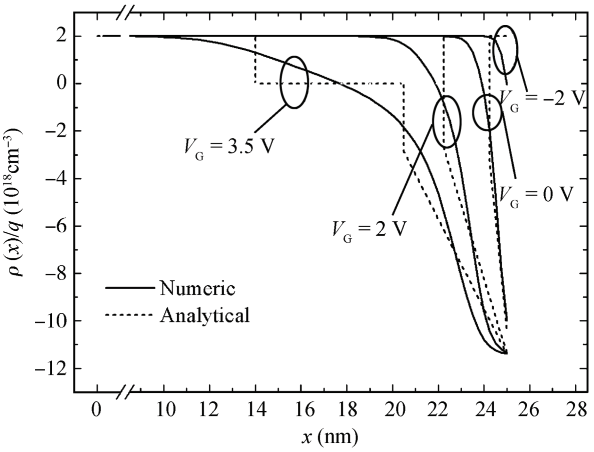

Fig. 4. Charge distribution in the AlGaN barrier layer for different gate biases.

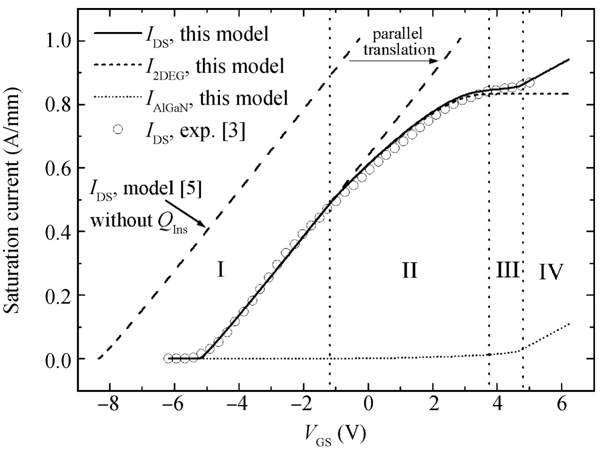

Fig. 6. Calculated and measured DC transfer characteristics.

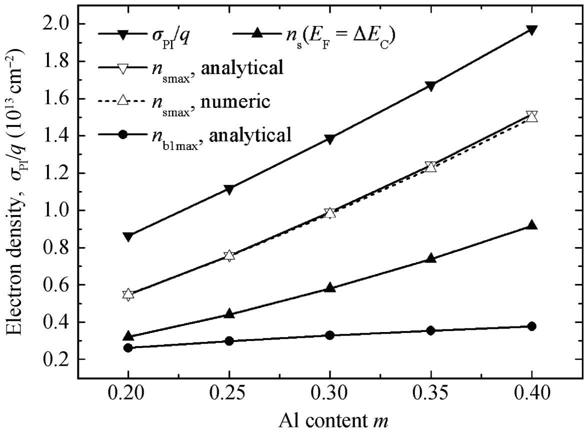

Fig. 5. Variation of σ_{PI}/q, n_s ($E_F = \Delta E_C$), n_{smax}, n_{b1max} with Al content.

strain relaxation, which results in the electron density dropping in the channel[16]. Thus, a compromise would be required for the optimal value of m.

Figure 6 shows the comparison between calculated DC transfer characteristics and experimental data[3]. On one hand, the fitted charge density at the insulator/AlGaN interface, Q_{Ins}/q, is about -3.33×10^{13} cm^{-2}, and it can cause a threshold voltage shift of 1.45 V, which illustrates its need to be taken into account in modeling. On the other hand, the span of region II accounts for about 50% of the gate voltage range before 2DEG saturates, which demonstrates the importance of considering the undepleted barrier layer. Comparing Figs. 6 and 3, it can be seen that though the quantity of free electrons is large in AlGaN at high gate voltage, its contribution to the total drain current is very small owing to the low electron mobility and saturation velocity. In Fig. 6, the good agreement between the analytical results and the measured data from the full depletion region to the electron accumulation region confirms the validity of the proposed model.

5. Conclusion

The whole charge control process of an AlGaN/GaN MIS-HFET is partitioned into four regions: I, full depletion; II, partial depletion; III, neutral region; and IV, electron accumulation at the insulator/AlGaN interface. For each region, an analytical charge control model is developed. The calculated transfer characteristic agrees reasonably well with the experimental data, which demonstrates the validity of the proposed model. The partitioning into four regions and the present model are helpful to understand the device physics, optimize the design and evaluate the performance.

References

[1] Wang Chong, Ma Xiaohua, Feng Qian, et al. Development and characteristics analysis of recessed-gate MOS HEMT. Journal of Semiconductors, 2009, 30(5): 054002

[2] Gregusova D, Stoklas R, Cico K, et al. AlGaN/GaN metal–oxide–semiconductor heterostructure field-effect transistors with 4 nm thick Al_2O_3 gate oxide. Semicond Sci Technol, 2007, 22: 947

[3] Yue Yuanzheng, Hao Yue, Feng Qian, et al. GaN MOS-HEMT using ultra-thin Al_2O_3 dielectric grown by atomic layer deposition. Chin Phys Lett, 2007, 24(8): 2419

[4] Maeda N, Hiroki M, Watanabe N, et al. Insulator engineering in GaN-based MIS HFETs. Proc SPIE, 2007, 6473: 647316

[5] Aggarwal R, Agrawal A, Gupta M, et al. Analytical performance evaluation of AlGaN/GaN metal insulator semiconductor heterostructure field effect transistor and its comparison with conventional HFETs for high power microwave applications. Microw Opt Technol Lett, 2008, 50(2): 331

[6] Lee K, Shur M S, Drummond T J, et al. Parasitic MESFET in (Al,Ga)As/GaAs modulation doped FET's and MODFET characterization. IEEE Trans Electron Devices, 1984, ED-31(1): 29

[7] Wang G W, Ku W H. An analytical and computer-aided model of the AlGaAs/GaAs high electron mobility transistor. IEEE Trans Electron Devices, 1986, 33(5): 657

[8] Ahn H, Nokali M E. An analytical model for high electron mobility transistors. IEEE Trans Electron Devices, 1994, 41(6): 874

[9] Aziz MA, El-Abd A. Theoretical study of the charge control in AlGaN/GaN HEMTs. NRSC, 2006: D6 1

[10] DasGupta A, DasGupta N. Simple analytical model for gate capacitance–voltage characteristics of HEMTs. Solid-State Electron, 1994, 37(7): 1377

[11] Ambacher O, Majewski J, Miskys C, et al. Pyroelectric properties of Al(In)GaN/GaN hetero- and quantum well structures. J Phys: Condens Matter, 2002, 14: 3399

[12] Pearton S J. Processing of wide band gap semiconductors. New York: William Andrew, 2000

[13] Yue Y, Hao Y, Zhang J, et al. AlGaN/GaN MOS-HEMT with HfO_2 dielectric and Al_2O_3 interfacial passivation layer grown by atomic layer deposition. IEEE Electron Device Lett, 2008, 29(8): 838

[14] Ambacher O, Smart J, Shealy J R, et al. Two dimensional electron gases induced by spontaneous and piezoelectric polarization charges in N- and Ga-face AlGaN/GaN heterostructures. J Appl Phys, 1999, 85(6): 3222

[15] ISE Integrated Systems Engineering AG. ISE TCAD Release 10.0, DESSIS, 2004

[16] Ambacher O, Foutz B, Smart J, et al. Two dimensional electron gases induced by spontaneous and piezoelectric polarization in undoped and doped AlGaN/GaN heterostructures. J Appl Phys, 2000, 87(1): 334